THE ASTROPHYSICAL JOURNAL, 457:13–18, 1996 January 20

STATISTICS OF ISODENSITY CONTOURS IN REDSHIFT SPACE

TAKAHIKO MATSUBARA
Department of Physics, University of Tokyo, Bunkyo-ku, Tokyo 113, Japan; matsu@utaphp1.phys.s.u-tokyo.ac.jp
Received 1994 September 12; accepted 1995 July 25

ABSTRACT

The peculiar velocities of galaxies distort the clustering pattern anisotropically in redshift space. This effect on the statistics of isodensity contours is examined by linear theory. The statistics considered in this paper are the three- and two-dimensional genera of isodensity contours, the area of isodensity contours, the length of isodensity contours in the two-dimensional slice, and the level crossing statistic on the line. We find that all these statistics in redshift space as functions of density threshold of contours have the same shape as in real space. The redshift space distortion affects only amplitudes of these statistics. The three-dimensional genus and the area hardly suffer from the redshift space distortion for $0 \leq \Omega b^{-5/3} \leq 1$, where b is a linear bias parameter. The other statistics are defined in one- or two-dimensional slices of the sample volume and depend on the direction of these slices relative to the line of sight. The latter statistics depend on $\Omega b^{-5/3}$. This dependence will be useful when the deep redshift surveys are available.

Subject headings: cosmology: theory — galaxies: distances and redshifts — large-scale structure of universe — methods: statistical

1. INTRODUCTION

Redshift surveys of galaxies play essential roles in revealing the structure of our universe. If galaxies move purely with the uniform Hubble expansion, redshift surveys would tell us the real distribution of galaxies. In reality, however, the peculiar velocities of galaxies distort the distribution in mapping from real space to redshift space. The distortion is along the line of sight, and the clustering pattern of galaxies in redshift space becomes anisotropic.

There are two characteristic features in the redshift space distortion. On very small scales, the random peculiar motions in virializing clusters stretch the shape of clusters along the line of sight, known as the "finger of God" effect. As a result, the strength of the clustering is weaker in redshift space than in real space (e.g., Lilje & Efstathiou 1989; Suto & Suginohara 1991; Peacock 1993; Matsubara 1994a). On large scales, the coherent velocity field falling in the region with the excess mass makes the perturbation enhanced along the line of sight, in contrast to the small-scale case (Sargent & Turner 1977; Kaiser 1987; Lilje & Efstathiou 1989; McGill 1990).

The redshift data are to be compared with many theories on the structure formation of the universe. The straightforward predictions of these theories, however, are usually described in real space. To compare the theories with observations, the various statistical measures, such as correlation functions, probability distribution functions, etc., are used. Among such statistics, there is a class of statistics using a smoothed density field which cuts the noisy property of galaxy distribution.

For example, Gott, Melott, & Dickinson (1986) introduced the topology of isodensity contours of those smoothed fields. The genus G, which is defined by $-\frac{1}{2}$ times the Euler characteristics of two-dimensional surfaces, can be a quantitative measure of the topology and was analyzed both in numerical simulations and in redshift surveys of galaxies by many authors (Gott, Weinberg, & Melott 1987; Weinberg, Gott, & Melott 1987; Melott, Weinberg, & Gott 1988; Gott et al. 1989; Park & Gott 1991; Park, Gott, & da Costa 1992; Weinberg & Cole 1992; Moore et al. 1992; Vogeley et al. 1994; Rhoads, Gott, & Postman 1994). Analytic expressions of the genus for some cases are already known, including the Gaussian random field (Doroshkevich 1970; Adler 1981; Bardeen et al. 1986; Hamilton, Gott, & Weinberg 1986), the Rayleigh-Lévy random-walk fractal (Hamilton 1988), union of overlapping balls (Okun 1990), and weakly non-Gaussian random fields (Matsubara 1994b). So far these expressions have been derived only for isotropic fields.

There are other statistics of isodensity contours, which include the two-dimensional genus in two-dimensional slices of density field G_2 (Melott et al. 1989), the area of isodensity contours N_3, the length of isodensity contours in two-dimensional slices of density field N_2, and the level crossing statistic N_1 (Ryden 1988; Ryden et al. 1989). The analytic expressions of all the above statistics for isotropic Gaussian random fields are known.

The growth of the density fluctuation of the universe on large scales is described by linear theory in the gravitational instability picture of the structure formation (e.g., Peebles 1980). Thus, if the initial fluctuation is a Gaussian random field, as is often assumed, the statistics of isodensity contours of the density field with large smoothing length should obey the random Gaussian prediction. Because the known analytic expression for Gaussian random fields is for the isotropic field, this Gaussianity test of the initial fluctuation should be performed in real space, which is not feasible in reality. It is not obvious whether or not the redshift space distortion strongly affects statistics of isodensity contours. As for the genus, Melott et al. (1988) found by analysis of N-body simulations that genus is hardly affected by redshift space distortion when the smoothing length is larger than the correlation length, ~ 5 h^{-1} Mpc.

In this paper, the redshift space distortions of statistics of isodensity contours G, G_2, N_3, N_2, and N_1 are studied analyti-

cally by linear theory of gravitational instability, assuming that the initial fluctuation is a Gaussian random field. These statistics will be determined accurately with the future redshift surveys. Our approach provides the Gaussianity test which can be performed directly in redshift space. Moreover, the redshift space distortion depends generally on the density parameter of the universe, and our formula could be expected to discriminate this parameter.

The rest of this paper is organized as follows. In § 2, the distant-observer approximation to evaluate the redshift space distortion of statistics is introduced. We show directly that our definition of this approximation is equivalent to the approximation adopted by Kaiser (1987), who gave for the first time the redshift space distortion of the two-point statistic by linear theory. Then we derive the useful anisotropic statistics in redshift space. The main results of this paper, the formulae for statistics of isodensity contours in redshift space, are derived in § 3. We discuss the results in § 4.

2. FIELD CORRELATIONS IN THE DISTANT-OBSERVER APPROXIMATION

Kaiser (1987) showed that the distortion of the power spectrum in redshift space, $P^{(s)}(\boldsymbol{k})$, from that in real space, $P^{(r)}(k)$, is given by the simple formula

$$P^{(s)}(\boldsymbol{k}) = (1 + f\mu^2)^2 P^{(r)}(k) , \tag{2.1}$$

where μ is the cosine of the angle between the line of sight and the direction of $\boldsymbol{k}$, and $f(\Omega) = H^{-1}\dot{D}/D \approx \Omega^{0.6}$, where D is the linear growth rate and H is the Hubble parameter. The Ω dependence of $f(\Omega)$ is approximately the same in the presence of cosmological constant Λ (for details see Lahav et al. 1991), and we use this approximation, $f \approx \Omega^{3/5}$, extensively in this paper. This simplicity of equation (2.1) relies on the approximation that the sample volume is distant enough from the observer compared with scales of fluctuations considered. Inhomogeneity of the redshift samples closer to the observer is not negligible, nor is the anisotropy; this prevents us from giving a simple expression as in equation (2.1). When the sample volume is distant from the observer, the direction of the line of sight is approximately fixed in the sample volume. We refer to this approximation fixing the line of sight as the "distant-observer approximation." Adopting this approximation, the Cartesian coordinates in which the line of sight is fixed are convenient for our purpose. The Cartesian coordinates make the calculation of statistics of isodensity contours easy. Our distant-observer approximation exactly reproduces Kaiser's result (eq. [2.1]), which is derived by first introducing spherical coordinates and then using the approximation that the sample is distant from the observer. Our approach depends on the Cartesian coordinates from the beginning, and it would be useful to see directly the equivalence of Kaiser's approximation and our distant-observer approximation. The derivation of Kaiser's result in Cartesian coordinates is simpler, as we will see in the following.

In the Cartesian coordinates of our distant-observer approximation we define the direction of the line of sight by a unit vector $\hat{z}$. Using the line-of-sight component of a peculiar velocity field $U(\boldsymbol{r}) = \boldsymbol{v}(\boldsymbol{r}) \cdot \hat{z}$, the mapping of the coordinates from real space to redshift space is given by

$$\boldsymbol{s}(\boldsymbol{r}) = \boldsymbol{r} + \frac{\hat{z}}{H}\left[U(\boldsymbol{r}) - U(\boldsymbol{0})\right] . \tag{2.2}$$

The observer is placed on the origin of the coordinates, $\boldsymbol{0}$. On the large scales we are interested in, we can relate the number density of galaxies in redshift space, $\rho_g^{(s)}$, and that in real space, $\rho_g^{(r)}$, by evaluating the Jacobian of the mapping in equation (2.2), resulting in

$$\rho_g^{(s)}[\boldsymbol{s}(\boldsymbol{r})] = \left[1 + \frac{1}{H}\hat{z} \cdot \nabla U(\boldsymbol{r})\right]^{-1} \rho_g^{(r)}(\boldsymbol{r}) . \tag{2.3}$$

Leaving only linear order in density contrast $\delta = \rho/\bar{\rho} - 1$ and peculiar velocity field, this relation reduces to

$$\delta_g^{(s)}(\boldsymbol{r}) = \delta_g^{(r)}(\boldsymbol{r}) - \frac{1}{H}\hat{z} \cdot \nabla U(\boldsymbol{r}) . \tag{2.4}$$

The peculiar velocity field in linear theory (Peebles 1980) is, in growing mode,

$$\boldsymbol{v}(\boldsymbol{r}) = -Hf\nabla\Delta^{-1}\delta_m^{(r)}(\boldsymbol{r}) , \tag{2.5}$$

where Δ^{-1} is the inverse Laplacian and $\delta_m^{(r)}$ is the mass density contrast in real space. In the following, δ_g and δ_m are assumed to be proportional to each other. This assumption is called linear biasing: $\delta_g = b\,\delta_m$, where b is the bias parameter which is a constant. The relation between the density contrast in redshift space and in real space is, up to linear order,

$$\delta_g^{(s)}(\boldsymbol{r}) = [1 + fb^{-1}(\hat{z} \cdot \nabla)^2\Delta^{-1}]\delta_g^{(r)}(\boldsymbol{r}) , \tag{2.6}$$

or, in Fourier space,

$$\tilde{\delta}_g^{(s)}(\boldsymbol{k}) = \left[1 + fb^{-1}\left(\frac{\hat{z} \cdot \boldsymbol{k}}{k}\right)^2\right]\tilde{\delta}_g^{(r)}(\boldsymbol{k}) , \tag{2.7}$$

which is Kaiser's result.

In the following, we use the parameters σ_j and C_j defined by

$$\sigma_j^2(R) = \int \frac{k^2\,dk}{2\pi^2}\,k^{2j}P^{(r)}(k)W^2(kR) , \tag{2.8}$$

$$C_j(\Omega) = \tfrac{1}{2}\int_{-1}^{1} d\mu\,\mu^{2j}(1 + fb^{-1}\mu^2)^2 , \tag{2.9}$$

where $W(x)$ is the Fourier transform of the window function to smooth the noisy field of the galaxy distribution. The two popular windows are the Gaussian window $W_G(x) = \exp(-x^2/2)$ and the top-hat window $W_{TH}(x) = 3(\sin x - x\cos x)/x^3$. We assume that the window function is an isotropic function. The rms $\sigma^{(s)}$ of density contrast in redshift space is given by

$$(\sigma^{(s)})^2 = C_0\,\sigma_0^2 . \tag{2.10}$$

We define the following normalized quantities,

$$\alpha = \frac{\delta_R^{(s)}}{\sigma^{(s)}} , \quad \beta_i = \frac{\partial_i\delta_R^{(s)}}{\sigma^{(s)}} , \quad \omega_{ij} = \frac{\partial_i\partial_j\delta_R^{(s)}}{\sigma^{(s)}} , \tag{2.11}$$

where $\delta_R^{(s)}$ is the smoothed density contrast in redshift space. These quantities obey the multivariate Gaussian distribution in linear theory if the primordial fluctuation is a random Gaussian field. The multivariate Gaussian distribution is determined completely by the correlations of all pairs of variables. For our purpose below, the statistics of quantities α, β_i, and ω_{IJ} ($i = 1, 2, 3$; $I, J = 1, 2$) is sufficient. Choosing the coordinates in which the line of sight is the third axis, all the correlations

among the above quantities at some point are as follows:

$$\langle \alpha\alpha \rangle = 1 , \quad \langle \alpha\beta_i \rangle = 0 ,$$

$$\langle \alpha\omega_{IJ} \rangle = \frac{1}{2}\left(\frac{C_1}{C_0} - 1\right)\frac{\sigma_1^2}{\sigma_0^2}\,\delta_{IJ} ,$$

$$\langle \beta_I \beta_J \rangle = \frac{1}{2}\left(1 - \frac{C_1}{C_0}\right)\frac{\sigma_1^2}{\sigma_0^2}\,\delta_{IJ} ,$$

$$\langle \beta_I \beta_3 \rangle = 0 , \quad \langle \beta_3 \beta_3 \rangle = \frac{C_1}{C_0}\frac{\sigma_1^2}{\sigma_0^2} , \quad \langle \beta_i \omega_{IJ} \rangle = 0 ,$$

$$\langle \omega_{IJ}\omega_{KL} \rangle = \frac{1}{8}\left(1 - \frac{2C_1}{C_0} + \frac{C_2}{C_0}\right)\frac{\sigma_2^2}{\sigma_0^2} \times (\delta_{IJ}\delta_{KL} + \delta_{IK}\delta_{JL} + \delta_{IL}\delta_{JK}) .$$

It is more convenient to consider

$$\tilde{\omega}_{IJ} = \omega_{IJ} - \alpha\langle \alpha\omega_{IJ} \rangle \tag{2.12}$$

instead of ω_{IJ}. The new set of variables α, β_i, and $\tilde{\omega}_{IJ}$ are distributed as multivariate Gaussian and the nonvanishing correlations of these variables are only

$$\langle \alpha\alpha \rangle = 1 ,$$

$$\langle \beta_1 \beta_1 \rangle = \langle \beta_2 \beta_2 \rangle = \frac{1}{2}\left(1 - \frac{C_1}{C_0}\right)\frac{\sigma_1^2}{\sigma_0^2} ,$$

$$\langle \beta_3 \beta_3 \rangle = \frac{C_1}{C_0}\frac{\sigma_1^2}{\sigma_0^2} ,$$

$$\langle \tilde{\omega}_{11}\tilde{\omega}_{11} \rangle = \langle \tilde{\omega}_{22}\tilde{\omega}_{22} \rangle = \frac{1}{8}\left[3\left(1 - \frac{2C_1}{C_0} + \frac{C_2}{C_0}\right) - 2\left(1 - \frac{C_1}{C_0}\right)^2\gamma^2\right]\frac{\sigma_2^2}{\sigma_0^2} ,$$

$$\langle \tilde{\omega}_{11}\tilde{\omega}_{22} \rangle = \frac{1}{8}\left[\left(1 - \frac{2C_1}{C_0} + \frac{C_2}{C_0}\right) - 2\left(1 - \frac{C_1}{C_0}\right)^2\gamma^2\right]\frac{\sigma_2^2}{\sigma_0^2} ,$$

$$\langle \tilde{\omega}_{12}\tilde{\omega}_{12} \rangle = \frac{1}{8}\left(1 - \frac{2C_1}{C_0} + \frac{C_2}{C_0}\right)\frac{\sigma_2^2}{\sigma_0^2} ,$$

where $\gamma = \sigma_1^2/(\sigma_0\sigma_2)$.

3. STATISTICS OF ISODENSITY CONTOURS

Let us derive the formula for statistics of isodensity contours in redshift space. In the following, the primordial fluctuation is assumed to be a random Gaussian field.

3.1. *Genus Statistic*

The genus is $-\frac{1}{2}$ times the Euler number. The Euler number density of isodensity contours is evaluated by

number of maxima + number of minima

− number of saddle points (3.1)

of the contour surfaces with regard to some fixed direction. The expectation value of the Euler number of the isodensity contours per unit volume is (Doroshkevich 1970; Adler 1981; Bardeen et al. 1986)

$$n_\chi^{(s)}(\nu) = \langle \delta(\alpha - \nu)\delta(\beta_1)\delta(\beta_2)\,|\,\beta_3\,|\,(\omega_{11}\omega_{22} - \omega_{12}^2)\rangle , \tag{3.2}$$

where the isodensity contours are defined to be the surface $\delta_R^{(s)} = \nu\sigma^{(s)}$. This expression is valid even for general anisotropic fields. Using new variables $\tilde{\omega}_{IJ}$ in equation (3.2), the following result for the expression of genus $G^{(s)}$ in redshift space is derived:

$$G^{(s)}(\nu) = -\frac{1}{2}\,n_\chi^{(s)}(\nu) = \frac{3\sqrt{3}}{2}\sqrt{\frac{C_1}{C_0}}\left(1 - \frac{C_1}{C_0}\right)G^{(r)}(\nu) , \tag{3.3}$$

where, from equation (2.9),

$$\frac{C_1}{C_0} = \frac{1}{3}\,\frac{1 + (6/5)fb^{-1} + (3/7)(fb^{-1})^2}{1 + (2/3)fb^{-1} + (1/5)(fb^{-1})^2} , \tag{3.4}$$

and $G^{(r)}$ is genus in real space (Doroshkevich 1970; Adler 1980; Bardeen et al. 1986; Hamilton et al. 1986) given by

$$G^{(r)}(\nu) = \frac{1}{(2\pi)^2}\left(\frac{\sigma_1}{\sqrt{3}\,\sigma_0}\right)^3(1 - \nu^2)e^{-\nu^2/2} . \tag{3.5}$$

The redshift space distortion does not alter the shape of genus as a function of density threshold, and only the amplitude is affected. The Ω dependence of the change in amplitude is plotted in Figure 1 (*top*). The effect of redshift space distortion is small for $\Omega b^{-5/3}$ less than unity. This fact is in agreement with the N-body analysis of Melott et al. (1988).

3.2. *Two-dimensional Genus Statistic*

The next statistic we consider is two-dimensional genus. This statistic is defined in the two-dimensional flat plane S in three-dimensional space. The density field calculated in three-dimensional volume defines the high-density points in the

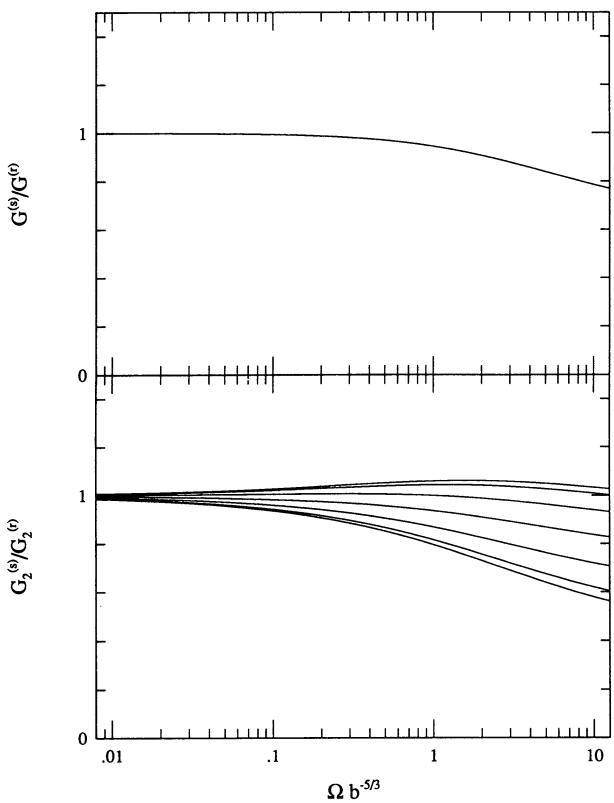

FIG. 1.—*Top:* amplitude of genus in redshift space relative to that in real space. *Bottom:* relative amplitude of two-dimensional genus. The angles between the slice and the line of sight are $\theta_S = 0°$, 15°, 30°, 45°, 60°, 75°, and 90° (*from upper line to lower line*).

plane which constitute the excursion set on the plane. The two-dimensional genus is defined by the number of contours surrounding the high-density region minus the number of contours surrounding low-density regions (Adler 1980; Coles 1988; Melott et al. 1989; Gott et al. 1990). The redshift space is anisotropic because of the presence of the special direction (line of sight), so the two-dimensional statistic depends on the angle θ_S between the plane S and the line of sight. The alternative, equivalent definition of two-dimensional genus is useful in the following. For some arbitrarily fixed direction in the two-dimensional surface, the maximum and minimum points are defined on the contours. These points are classified into upcrossing and downcrossing points with respect to the fixed direction. The two-dimensional genus is defined to be

$$\tfrac{1}{2}\,(\text{number of upcrossing minima} - \text{number of upcrossing maxima} - \text{number of downcrossing minima} + \text{number of downcrossing maxima}) \quad (3.6)$$

of the contour lines with regard to some fixed direction in the plane S. The latter definition can be used to obtain the following expression for two-dimensional genus per unit area of the plane:

$$G_2^{(s)}(\nu, \theta_S) = -\tfrac{1}{2}\langle\delta(\alpha-\nu)\delta(\beta_1)\,|\,\beta_2 \sin\theta_S + \beta_3\cos\theta_S\,|\,\omega_{11}\rangle\,. \quad (3.7)$$

The corresponding expression in the case of the isotropic two-dimensional field appeared in Bond & Efstathiou (1987). From this expression, we obtain

$$G_2^{(s)}(\nu, \theta_S) = \frac{3}{2}\sqrt{\left(1-\frac{C_1}{C_0}\right)\left[1-\frac{C_1}{C_0}+\left(\frac{3C_1}{C_0}-1\right)\cos^2\theta_S\right]} \times G_2^{(r)}(\nu)\,. \quad (3.8)$$

To derive this result, we use $\tilde{\omega}_{11}$ rather than ω_{11}, then regard the variables α, β_1, $\beta_2 \sin\theta_S + \beta_3\cos\theta_S$, and $\tilde{\omega}_{11}$ as independent variables. The two-dimensional genus in real space $G_2^{(r)}$ has the following form:

$$G_2^{(r)}(\nu) = \frac{1}{(2\pi)^{3/2}}\left(\frac{\sigma_1}{\sqrt{3}\,\sigma_0}\right)^2 \nu e^{-\nu^2/2}\,. \quad (3.9)$$

The redshift space distortion again affects only the amplitude of two-dimensional genus. The dependence on Ω and θ_S of the change in amplitude is plotted in Figure 1 (*bottom*). The dependence on the direction of the plane θ_S for large Ω can be used to determine the cosmological parameter by this statistic.

3.3. *Area of Isodensity Contours*

The area of isodensity contours per unit volume (Ryden 1988; Ryden et al. 1989) is given by

$$N_3^{(s)}(\nu) = \langle\delta(\alpha-\nu)\sqrt{\beta_1^2+\beta_2^2+\beta_3^2}\rangle\,. \quad (3.10)$$

This expression is valid even for general anisotropic fields. Introducing spherical coordinates for β_i, the above expression is calculated to be

$$N_3^{(s)}(\nu) = \frac{\sqrt{3}}{2}\left\{\sqrt{\frac{C_1}{C_0}} - \left(1-\frac{C_1}{C_0}\right)\Big/\left[2\sqrt{2\left(\frac{3C_1}{C_0}-1\right)}\right] \times \ln\left|\left[\sqrt{\frac{C_1}{C_0}} - \sqrt{\frac{1}{2}\left(\frac{3C_1}{C_0}-1\right)}\right]\Big/\left[\sqrt{\frac{C_1}{C_0}} + \sqrt{\frac{1}{2}\left(\frac{3C_1}{C_0}-1\right)}\right]\right|\right\} \times N_3^{(r)}(\nu)\,, \quad (3.11)$$

where $N_3^{(r)}$ is the area in real space given by

$$N_3^{(r)}(\nu) = \frac{2}{\sqrt{3\pi}}\frac{\sigma_1}{\sigma_0}e^{-\nu^2/2}\,. \quad (3.12)$$

Again, only the amplitude is affected. The Ω dependence of the amplitude is very weak as plotted in Figure 2 (*top*).

3.4. *Length of Isodensity Contours in Planes*

As in the case of the two-dimensional genus statistic, a two-dimensional flat plane S is considered in the statistic of length of isodensity contours. The length of intersections of isodensity contours and the plane S was introduced by Ryden (1988). For isotropic density fields, this statistic is proportional to the area of statistic considered in the previous section. As shown below, for anisotropic fields in redshift space, the proportionality factor depends on the direction of the surface S relative to the line of sight. The angle θ_S between the plane S and the line of sight is relevant as in the case of the two-dimensional genus statistic. The expectation value of length of isodensity contours in the plane S per unit area of the plane is given by

$$N_2^{(s)}(\nu, \theta_S) = \langle\delta(\alpha-\nu)\sqrt{\beta_1^2 + (\beta_2\sin\theta_S + \beta_3\cos\theta_S)^2}\rangle\,. \quad (3.13)$$

To evaluate the above equation, note that α, β_1, and $\beta_2 \sin\theta_S + \beta_3\cos\theta_S$ are noncorrelated, independent variables. Introducing the polar coordinates for the latter two variables, the

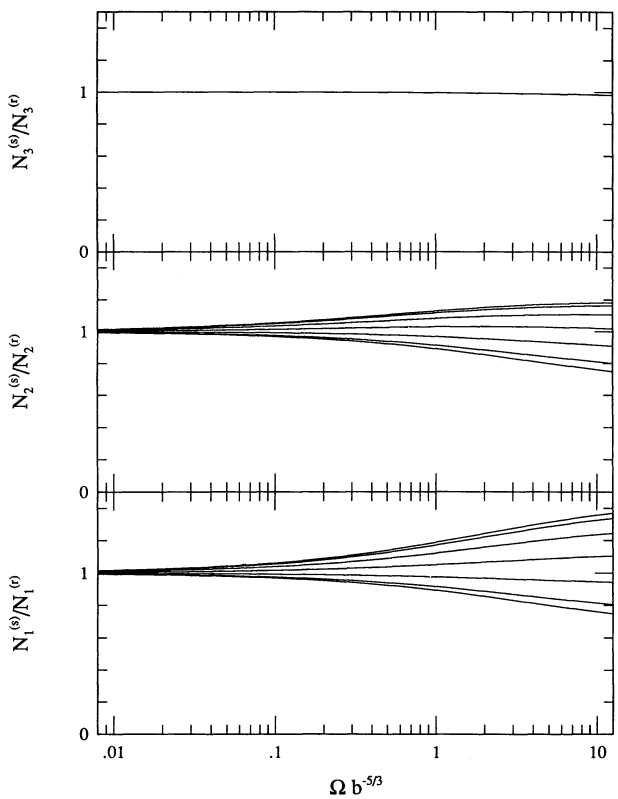

FIG. 2.—*Top:* amplitude of area statistic in redshift space relative to that in real space. *Middle:* relative amplitude of length statistic. The angles between the slice and the line of sight are $\theta_S = 0°$, 15°, 30°, 45°, 60°, 75°, and 90° (*from upper line to lower line*). *Bottom:* relative amplitude of level crossing statistic. The angles between the crossing line and the line of sight are $\theta_L = 0°$, 15°, 30°, 45°, 60°, 75°, and 90° (*from upper line to lower line*).

following expression is obtained:

$$N_2^{(s)}(\nu, \theta_S) = \frac{\sqrt{6}}{\pi}\sqrt{1 - \frac{C_1}{C_0} + \left(\frac{3C_1}{C_0} - 1\right)\cos^2\theta_S} \times E\left(\frac{[(3C_1/C_0) - 1]\cos^2\theta_S}{1 - (C_1/C_0) + [(3C_1/C_0) - 1]\cos^2\theta_S}\right) \times N_2^{(r)}(\nu)\,, \quad (3.14)$$

where $E(k)$ is the complete elliptical integral of the second kind,

$$E(k) = \int_0^{\pi/2}\sqrt{1 - k^2\sin^2\phi}\,d\phi\,, \quad (3.15)$$

and $N_2^{(r)}$ is the expectation in real space,

$$N_2^{(r)}(\nu) = \frac{\pi}{4}N_3^{(r)}\,. \quad (3.16)$$

The redshift space distortion affects only amplitude as well as other statistics considered in this paper. The dependence on Ω and θ_S of the amplitude is plotted in Figure 2 (*middle*).

3.5. *Contour Crossings*

The contour crossing statistic is the mean number of intersections of a straight line L and the isodensity contours. This statistic of large-scale structure is introduced by Ryden (1988) and studied extensively by Ryden et al. (1989) using numerical simulations and redshift observations. For isotropic density fields, this statistic is also proportional to the area statistic. In redshift space, the density field is anisotropic, and this statistic depends on the angle θ_L between the direction of the line L and the line of sight. The mean number of crossings per unit length of the line L is given by

$$N_1^{(s)}(\nu, \theta_L) = \langle\delta(\alpha - \nu)|\beta_1\sin\theta_L + \beta_3\cos\theta_L|\rangle\,. \quad (3.17)$$

This expression is evaluated by noting that α and $\beta_1\sin\theta_L + \beta_2\cos\theta_L$ are noncorrelated, independent variables, resulting in

$$N_1^{(s)}(\nu, \theta_L) = \sqrt{\frac{3}{2}\left[1 - \frac{C_1}{C_0} + \left(\frac{3C_1}{C_0} - 1\right)\cos^2\theta_L\right]}N_1^{(r)}(\nu)\,, \quad (3.18)$$

where $N_1^{(r)}$ is the expectation in real space,

$$N_1^{(r)}(\nu) = \tfrac{1}{2}N_3^{(r)}(\nu)\,. \quad (3.19)$$

Again, the redshift space distortion affects only amplitude. The dependence of the amplitude on Ω and θ_L is plotted in Figure 2 (*bottom*).

4. DISCUSSION

The strength of the effects of redshift space distortion varies according to which statistic is focused on. The characteristic point in linear theory is that all the statistics in redshift space considered in this paper have the same shapes as in real space as functions of density threshold. The redshift space distortion affects only the amplitude.

As for genus $G(\nu)$ and area $N_3(\nu)$, the redshift distortion of amplitude is small for $0 \le \Omega b^{-5/3} \le 1$ (Figs. 1–2). This property justifies the comparison of the observational redshift data and the theoretical Gaussian prediction in real space (eqs. [3.5] and [3.12]), at least in the linear regime. In the Gaussianity test of primordial fluctuation using genus and area statistics, the effect of redshift space distortion can be ignored approximately. The similar statistical measure of galaxy clustering, the skewness $\langle\delta_R^3\rangle/\langle\delta_R^2\rangle^2$ induced by weakly nonlinear evolution from the Gaussian primordial fluctuation, has recently been reported not to be affected much by redshift space distortion (Juszkiewicz, Bouchet, & Colombi 1993; Hivon et al. 1994).

The direction-dependent statistics, two-dimensional genus G_2, length statistic N_2, and crossing statistic N_1, are shown to exhibit the dependence on Ω and the direction to define statistics. In Figure 3, the direction dependence of these three statistics is plotted. The direction dependence of amplitude on these statistics is relatively large: for $\Omega b^{-5/3} = 1$, the amplitude varies more than 20%, while for $\Omega b^{-5/3} = 0$, the amplitude does not vary and is equal to the amplitude in real space. The direction dependence depends on $\Omega b^{-5/3}$, and the statistics G_2, N_2, and N_1 are three different types of indicators to determine the cosmological parameters. The redshift space distortion of the power spectrum (eq. [2.1]) or the two-point correlation function of Kaiser's result were used for determining the parameter $\Omega b^{-5/3}$ (Hamilton 1992, 1993; Fry & Gaztañaga 1994; Cole, Fisher, & Weinberg 1994). Gramann, Cen, & Gott (1994) introduced the ratio of density gradients $\langle[\partial\delta^{(s)}/\partial r_\parallel]^2\rangle/\langle[\partial\delta^{(s)}/\partial r_\perp]^2\rangle$ as a discriminator of $\Omega b^{-5/3}$, where $r_\parallel$ is a coordinate which is parallel to the line of sight and $r_\perp$ is a coordinate which is perpendicular to the line of sight. This ratio is equal to $3C_1/C_0$ in linear theory. Our results can be used as a complement to these observations.

However, there are some caveats on the results. Linear theory is valid on fairly large scales. Our results are valid when

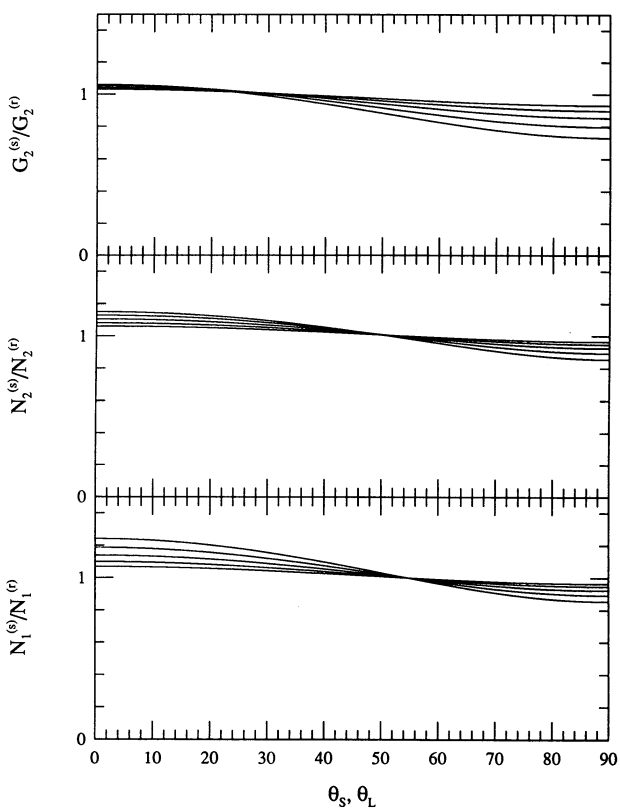

FIG. 3.—Relative amplitude of direction-dependent statistics as functions of the angle between the line of sight and the plane or the line on which the statistics are evaluated. Five cases $\Omega b^{-5/3} = 0.125, 0.25, 0.5, 1.0$, and 2.0 (*from upper line to lower line at* $\theta = 90°$) are plotted in each panel. *Top:* two-dimensional genus. *Middle:* length statistic. *Bottom:* level crossing statistic.

the smoothing length R is large enough to guarantee $\sigma_0 \ll 1$. This means that we should take $R \gg 8\ h^{-1}$ Mpc. We need a large smoothing length, greater than ~ 10–$20\ h^{-1}$ Mpc, for the comparison with observations. This is too large, however, to have statistical significance for the presently available data. This is a limitation of our analysis if the redshift sample is not so deep.

When smoothing length is not very large and σ_0 is not much less than unity, there are still nonlinear effects. As for the genus statistic, we find that the amplitude of the genus curve is suppressed more than that expected in linear theory (Matsubara & Suto 1996) from the comparison with N-body simulations. Nonlinear evolution changes the shape of the genus curve or of curves of other statistics of isodensity contours (Matsubara 1994b, 1995). The N-body result shows that the shape of the genus curve in redshift space is still the same as in real space in the weakly nonlinear regime ($\sigma_0 \lesssim 1$).

Strictly speaking, our results should be applied to very deep samples, such as the Sloan Digital Sky Survey, to have a sufficient level of statistical significance. As the sample depth of the galaxy redshift survey increases, the redshift distortion attributable to the cosmological expansion or general relativistic effect becomes important (Alcock & Paczyński 1979; Ryden 1995). In the Friedmann-Lemaître model, the comoving distance to the object at z is given by

$$d_C = \frac{c}{H_0}\begin{cases} (\Omega_0 + \lambda_0 - 1)^{-1/2} \sin\left(\chi\sqrt{\Omega_0 + \lambda_0 - 1}\right) & \text{for } \Omega_0 + \lambda_0 > 1\ , \\ \chi & \text{for } \Omega_0 + \lambda_0 = 1\ , \\ (1 - \Omega_0 - \lambda_0)^{-1/2} \sinh\left(\chi\sqrt{1 - \Omega_0 - \lambda_0}\right) & \text{for } \Omega_0 + \lambda_0 < 1\ , \end{cases} \tag{4.1}$$

where

$$\chi \equiv \int_0^z [\Omega_0(1+z)^3 + (1 - \Omega_0 - \lambda_0)(1+z)^2 + \lambda_0]^{-1/2}\, dz\ . \tag{4.2}$$

For $z \ll 1$, d_C is given approximately by

$$d_C = \frac{cz}{H_0}\left[1 + \frac{2\lambda_0 - \Omega_0 - 2}{4}\, z + O(z^2)\right]. \tag{4.3}$$

Therefore, the deviation from the simple linear Hubble law becomes appreciable even at relatively low z; at $z = 0.1$ ($\sim 300\ h^{-1}$ Mpc), the *cosmological redshift space distortion* becomes -7.5% in the Einstein–de Sitter model. Thus, even for redshift surveys extending up to $z = 0.1$, this systematic effect dominates the statistical peculiar velocity effect ($\sim 3\%$ for $v = 1000$ km s^{-1} at $z = 0.1$, for instance). One can compute the statistics of the observed sample in d_C space rather than in z space using equation (4.1) directly. In any case, the result should be sensitive to the assumed set of Ω_0 and λ_0. In this case, some feedback procedure is needed to distinguish low Ω and high Ω using Figure 3. Note, however, that this problem is not specific to the statistics of isodensity contours, but it should be taken into account in the two-point and higher order correlation analyses as well.

I am grateful to Y. Suto for a careful reading of the manuscript and useful comments. Thanks are also due to the referee, B. Ryden, for pointing out the importance of the cosmological redshift space distortion in the present study. I acknowledge the support of a JSPS Fellowship. This research was supported in part by grants-in-aid for scientific research from the Ministry of Education, Science, and Culture of Japan (No. 0042).

REFERENCES

Adler, R. J. 1981, The Geometry of Random Fields (Chichester: Wiley)
Alcock, C., & Paczyński, B. 1979, Nature, 281, 358
Bardeen, J. M., Bond, J. R., Kaiser, N., & Szalay, A. S. 1986, ApJ, 304, 15
Bond, J. R., & Efstathiou, G. 1987, MNRAS, 226, 655
Cole, S., Fisher, K. B., & Weinberg, D. H. 1994, MNRAS, 267, 785
Coles, P. 1988, MNRAS, 234, 509
Doroshkevich, A. G. 1970, Astrophysics, 6, 320 (transl. from Astrofizika, 6, 581)
Fry, J. N., & Gaztañaga, E. 1994, ApJ, 425, 1
Gott, J. R., Melott, A. L., & Dickinson, M. 1986, ApJ, 306, 341
Gott, J. R., et al. 1989, ApJ, 340, 625
Gott, J. R., Park, C., Juszkiewicz, R., Bies, W. E., Bennett, D. P., Bouchet, F. R., & Stebbins, A. 1990, ApJ, 352, 1
Gott, J. R., Weinberg, D. H., & Melott, A. L. 1987, ApJ, 319, 1
Gramann, M., Cen, R., & Gott, J. R. 1994, ApJ, 425, 382
Hamilton, A. J. S. 1988, PASP, 100, 1343
———. 1992, ApJ, 385, L5
———. 1993, ApJ, 406, L47
Hamilton, A. J. S., Gott, J. R., & Weinberg, D. 1986, ApJ, 309, 1
Hivon, E., Bouchet, F. R., Colombi, S., & Juszkiewicz, R. 1994, preprint
Juszkiewicz, R., Bouchet, F. R., & Colombi, S. 1993, ApJ, 412, L9
Kaiser, N. 1987, MNRAS, 227, 1
Lahav, O., Lilje, P. B., Primack, J. R., & Rees, M. J. 1991, MNRAS, 251, 128
Lilje, P. B., & Efstathiou, G. 1989, MNRAS, 236, 851
Matsubara, T. 1994a, ApJ, 424, 30
———. 1994b, ApJ, 434, L43
———. 1995, in Proc. 11th Potsdam Cosmology Workshop, Large Scale Structure in the Universe—Theoretical and Observational Aspects, ed. J. Muecket (Singapore: World Scientific), in press
Matsubara, T., & Suto, Y. 1996, ApJ, submitted
McGill, C. 1990, MNRAS, 242, 428
Melott, A. L., Cohen, A. P., Hamilton, A. J. S., Gott, J. R., & Weinberg, D. H. 1989, ApJ, 345, 618
Melott, A. L., Weinberg, D. H., & Gott, J. R. 1988, ApJ, 328, 50
Moore, B., et al. 1992, MNRAS, 256, 477
Okun, B. L. 1990, J. Stat. Phys., 59, 523
Park, C., & Gott, J. R. 1991, ApJ, 378, 457
Park, C., Gott, J. R., & da Costa, L. N. 1992, ApJ, 392, L51
Peacock, J. A. 1993, in Proc. Valencia Summer School, New Insights into the Universe, ed. V. J. Martinez (Berlin: Springer), 1
Peebles, P. J. E. 1980, The Large-Scale Structure of the Universe (Princeton: Princeton Univ. Press)
Rhoads, J. E., Gott, J. R., & Postman, M. 1994, ApJ, 421, 1
Ryden, B. S. 1988, ApJ, 333, L41
———. 1995, ApJ, 452, 25
Ryden, B. S., Melott, A. L., Craig, D. A., Gott, J. R., Weinberg, D. H., Scherrer, R. J., Bhavsar, S. P., & Miller, J. M. 1989, 340, 647
Sargent, W. L. W., & Turner, E. L. 1977, ApJ, 212, L3
Suto, Y., & Suginohara, T. 1991, ApJ, 370, L15
Vogeley, M. S., Park, C., Geller, M. J., Huchra, J. P., & Gott, J. R. 1994, ApJ, 420, 525
Weinberg, D. H., & Cole, S. 1992, MNRAS, 259, 652
Weinberg, D. H., Gott, J. R., & Melott, A. L. 1987, ApJ, 321, 2